Available online at www.sciencedirect.com
ScienceDirect
Journal of Nuclear Materials 367–370 (2007) 344–349
journal of nuclear materials
www.elsevier.com/locate/jnucmat

Identification and characterization of defects produced in irradiated fused silica through molecular dynamics

F. Mota [a,*], M.-J. Caturla [c], J.M. Perlado [a], A. Ibarra [b], M. León [b], J. Mollá [b]

[a] Universidad Politécnica de Madrid, ETSII, Instituto de Fusion Nuclear, C/ Jose Gutierrez Abascal 2, CP: 28006 Madrid, Spain
[b] Materiales para Fusion, Ciemat, Avda complutense 22, Madrid 28040, Spain
[c] Universidad de Alicante, Dep. Fisica Aplicada, Alicante, Spain

Abstract

We present molecular dynamics simulations of displacement cascades due to energetic recoils in amorphous silica, a candidate material for fusion applications. We have performed a statistical study of the different kinds of defects produced as a function of primary knock-on atom (PKA) energy. The range of energies studied is from 0.4 to 3.5 keV. We measure how the concentration of different kinds of defects vary with recoil energy and we catalogue these defect according to their potential energy, morphology and coordination. Our calculations show mainly four types of defects, Si_3, Si_5, O_1 and O_3 where the numbers denote their coordination. The production of these defects increases with PKA energy except for the case of Si_5. A faster increase in the production rate with energy is observed for O_1 and O_3 types of defects with respect to Si_3. Results are correlated to known experimentally observed defects.

1. Introduction

Fused silica is a candidate material for optical and radio-frequency diagnostic systems in magnetic confinement fusion reactors [1] and as final optics in inertial confinement fusion reactors [2]. In both cases this material will be exposed to high energy neutron (14 MeV) and gamma irradiation. Radiation induces optical absorption, creating point defects that can act as colour centers [3]. One of the defects observed experimentally after neutron irradiation is the oxygen deficient center (ODC) [3,4]. Its conversion to E' centers after gamma irradiation has been observed by some studies [3].

In this work we study the production of point defects due to atomic displacements, such as those produced by neutron irradiation. We center this study on characterizing the types of defects produced during irradiation based on the coordination and potential energy of all the atoms in the simulation box after each collision event. In terms of the applications of interest, namely fusion reactor materials, the most important defect that has been identified experimentally is a colour center in the 248 nm wavelength. This defects, which appears under neutron irradiation and makes the material opaque [1,2], is the so-called oxygen deficient center (ODC). Under gamma irradiation this defect is converted to E' centers with a 214 nm wavelength according to

* Corresponding author. Tel.: +34 91 336 3108; fax: +34 91 336 3002.
E-mail address: mota@denim.upm.es (F. Mota).

0022-3115/$ - see front matter © 2007 Published by Elsevier B.V.
doi:10.1016/j.jnucmat.2007.03.130

some studies [3]. However, other types of defects are also produced during irradiation, some of which have not been identified yet. Our previous calculations have focused primarily on ODCs [5,6]. In this study we also identify other possible defects produced during irradiation and compare to the experimentally observed ones.

2. Simulation modeling

We use molecular dynamics simulations to study the defects produced in fused silica. Fused silica is an amorphous system, formed by silicon atoms tetrahedrally bonded to oxygen atoms. The interatomic potential used for our calculations is the one developed by Feuston and Garofalini [7], a potential that was fitted to reproduce the structure factor of this amorphous system as determined experimentally through X-ray diffraction and neutron scattering data. In order to generate the amorphous system of fused silica, we start with a crystal lattice of beta-cristobalite for SiO_2 because its structure is very similar in its short range order (tetrahedral structure SiO_4^{-4}). This structure is melted (at 7000 K) and quenched through a series of steps until a final temperature of 300 K is achieved. Simulations have been performed using a parallel molecular dynamics code MDCASK [8]. Indicators of the amorphous structure such as the structure factor, the bond angle distribution, coordination or ring statistics are computed in order to check the final structure of the computational box [7,9]. The simulation box size used had 192 000 atoms, that is approximately $15 \times 15 \times 15\ nm^3$ in size.

Once the initial amorphous structure is constructed and cooled to room temperature (300 K), we identify the defects in the bulk. Periodic boundary conditions are used with a bath control to keep the final temperature at 300 K through scaling the velocities of those atoms close to the border of the simulation box. An energetic silicon atom is chosen in the center of the simulation box for low PKA energy and in the top of the box when the PKA energy is higher.

3. Results

Identification of defects in an amorphous system is quite complex. Unlike in perfect crystals, the identification is not unique, therefore a definition of point defect must be described. For each atom in our lattice, we determine its coordination by employing a cut-off radius of 2.15 Å which lies between the first and second nearest neighbor distance (this distance is the minimum between first and second nearest neighbors distance in the pair correlation function [7,10]).

In addition, we cataloged different kinds of defects by the potential energy. When the potential energy of all atoms in the lattice is grouped and plotted, there is a clear separation between the different types of defects, as shown in Fig. 1, since this energy depends on the coordination of the atoms. In this graph we have plotted the number of Si and O atoms with any given potential energy. The coordination of each atom has also been calculated. Si_4 and O_2 represent perfect coordinated silicon and oxygen atoms in fused silica, respectively, while the rest are either over or under coordinated Si and O atoms, and therefore correspond to defects in the fused silica matrix. A clear correlation is observed between the coordination of the atoms and the range of possible potential energies. Fig. 1 corresponds to a box size of 192 000 atoms and a temperature of 300 K. Fig. 1(a) is before the displacement cascade and Fig. 1(b) is during the displacement cascade 6 fs after the initial collision.

The defects that appear in Fig. 1 can be explained as follows:

1. Si_3: Silicon with 3 oxygens as nearest neighbors. To compare the Si_3 with the literature, it corresponds to an oxygen vacancy or oxygen deficient center (ODC). An E' center is also an oxygen vacancy, but it has an unpaired electron. However, within our simulation framework such a distinction can not be made. As shown in Figs. 1(a) and (b) the Si_3 has a range of potential energies between (−25.05 eV: −24.55 eV) before the cascade collision while after 6 fs for one cascade of 1.5 keV the range of energies grow significantly (−26.65 eV:−16,85 eV).
2. Si_5: Silicon with coordination 5: silicon with 5 oxygens as nearest neighbors. In Fig. 1(a) we can see that the range of energies is (−30.25 eV: −27.95 eV) before irradiation and (−30.45 eV: −24.9 eV) at 6 fs.
3. O_1: Oxygen with coordination 1: one silicon as nearest neighbor. This defect is similar to the non-bridging oxygen (NBOs) in the literature [3]. The range of potential energy Fig. 1(a) is (−7.85 eV:−4.2 eV), and in Fig. 1(b) (−14.1 eV: −9.3 eV).

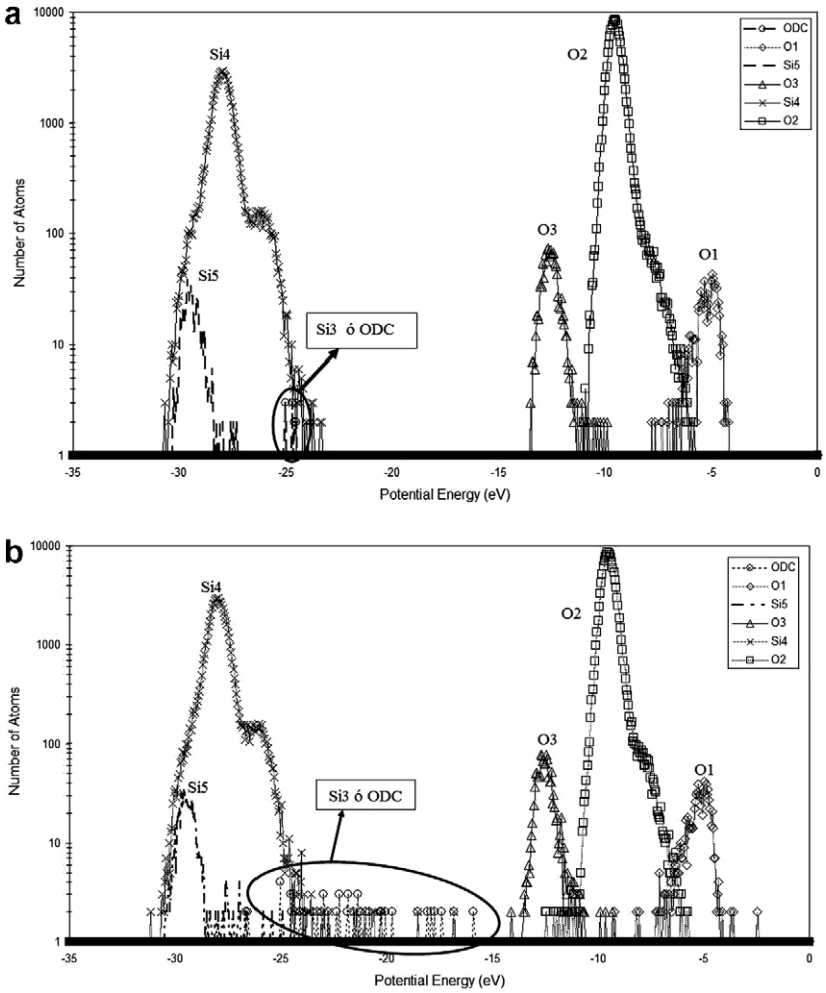

Fig. 1. Potential energy spectrum of atoms with different coordination. (a) Before the displacement cascade and (b) during the displacement cascade 6 fs after the initial collision.

4. O_3: Oxygen with coordination 3, oxygen with 3 silicon as nearest neighbors. The range of potential energy in Fig. 1(a) is (−13.5 eV:−11.15 eV), and in Fig. 1(b) (−14.1 eV:−9.3 eV). In addition, we obtained the spectrum of energy for both silicon and oxygen atoms perfectly coordinated.
5. Si_4: Silicon with coordination 4 (perfect coordination). In Fig. 1(a) the range of potential energy is (−30.7 eV:−23.35 eV) and in Fig. 1(b) (−31.15 eV:−22.75 eV).
6. O_2: Oxygen with coordination 2 (perfect coordination). In Fig. 1(a) the range of potential energy is (−11.0 eV:−5.8 eV) and in Fig. 1(b) (−12.5 eV: −5.75 eV). A description of the atomic and morphology configurations these defects can be found in Ref. [11].

Fig. 2 shows the difference between the potential energy of atoms before the collision cascade and after the collision cascade (4.5 ps) for the same cascade of Fig. 1 (1.5 keV). This difference shows the actual stable defects produced in the cascade. It is clear from this figure that each defect has a defined range of potential energies and that this range does not change during the cascade production except for the case of the Si_3. For this last defect there is a wide range of potential energies, however no other type of defect falls in the same potential energy range. This wide range of energies persists only at the peak of the collision cascade and it is greatly reduced after the cascade collapse.

For the initial amorphous structure used in these calculations the percentage of Si_3 with respect to the

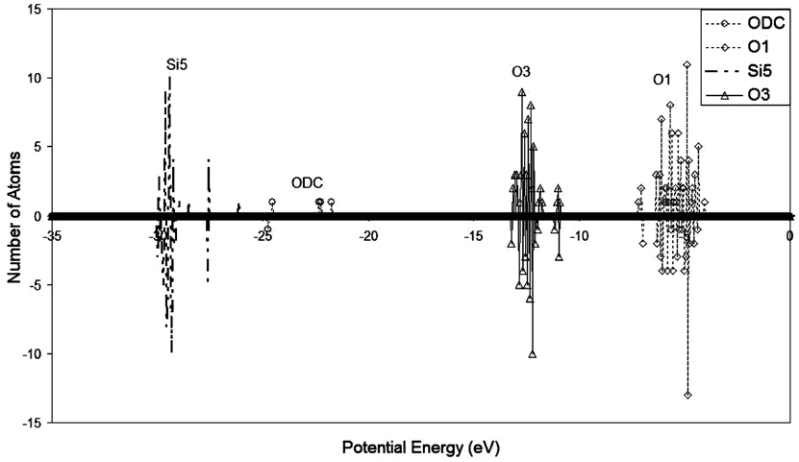

Fig. 2. Difference between the potential energy in the initial situation (before collision cascade) and after cascade collapse.

total number of silicon atoms is 0.009% and of Si_5 is 0.748%. The percentage of O_1 with respect to the total oxygen atoms is 0.570% and of O_3 is 0.939%. Therefore, we start with an initial concentration of O_3, Si_5 and O_1 defects and a much lower concentration of Si_3. These numbers are in agreement of those reported by Feuston and Garofalini [5].

We have analysed a PKA energy range from 400 eV to 3.5 keV. For each energy value, we have performed several cascade simulations, since it is necessary to do an average to get a statistical value of the number of defects produced. In principle the variations in an amorphous material can be larger than in a crystalline sample. It will depend on the location of the energetic atom chosen, since not all positions are equivalent. In this study we have made the average from five different cases of each energy.

Fig. 3 shows the results of the average of number of generated defects (Si_3, Si_5, O_1, and O_3) versus PKA energy. The simulation is followed for a total time of 4.5 ps using a time step of 0.1 fs, but the variation system of time step is used to assure that the time step used is enough for each displacement cascade time. The time step is varied in function of movement of atoms. After each simulation we remove the thermal fluctuation to determine the stable defects. The method used consists in searching for those atoms that move towards equilibrium. If the atom moves away from equilibrium its velocity is fixed but if the atom moves towards equilibrium

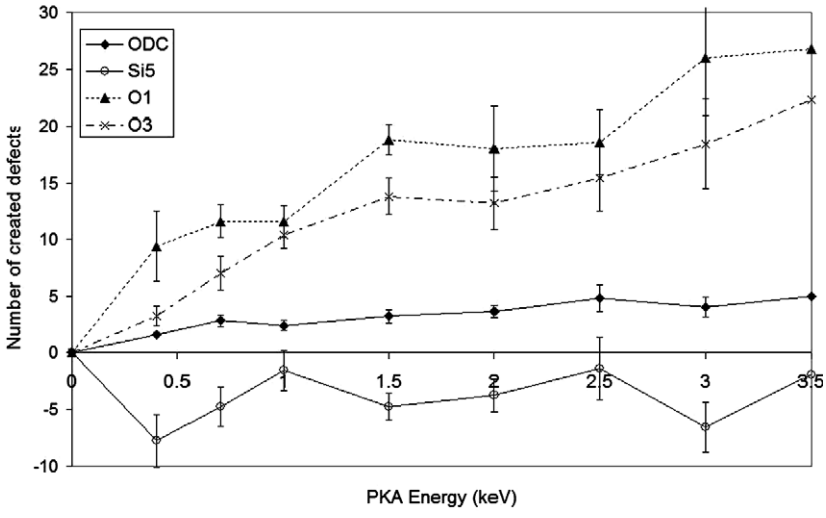

Fig. 3. Average of number of generated defects (Si_3, Si_5, O_1, and O_3) versus PKA energy.

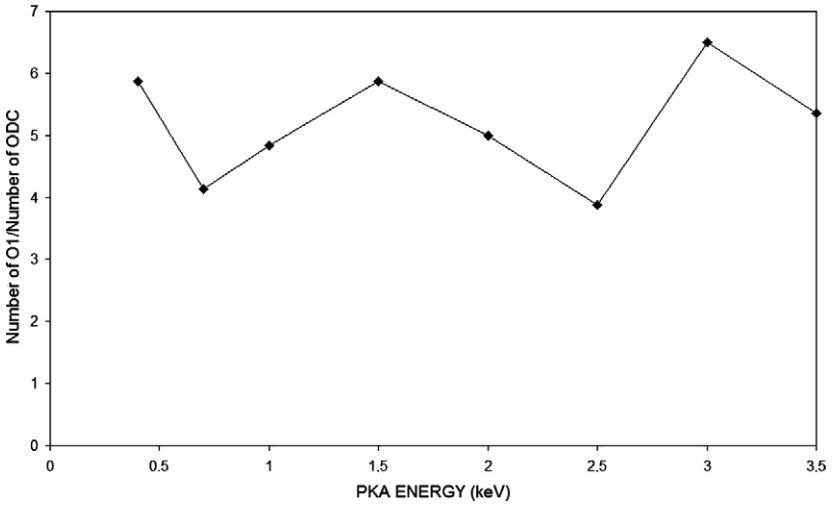

Fig. 4. Ratio of number of O_1 to number of Si_3 defects.

its velocity is not changed. This process quenches the system removing the thermal vibrations. The number of defects plotted in Fig. 3 was obtained by substracting from the final number of defects after the collision cascade and quenched lattice (removing the thermal fluctuations) the initial number of defects in the lattice. This is performed for every simulation and averaged over all the calculations at each energy.

In Fig. 3 we can clearly see that the number of defects Si_3, O_1 and O_3 grow with PKA energy. The rate of increase of O_1 and O_3 defect production with PKA energy is higher than for the case of Si_3. In addition it can be seen that the number of Si_5 is not affected with the variation of PKA energy, at least up to the highest energy studied here, 3.5 keV. Moreover, the values of Si_5 after the cascade collapse are negative meaning that due to the collision cascade some of these defects are healed. Interestingly the number of healed defects is independent of cascade energy.

Fig. 4 shows the ratio between the number of O_1 and Si_3 defects for each energy. It is interesting that this ratio is practically constant for all energies. However, its value is higher than 1, which would correspond to bond breaking and special correlation between these two defects.

4. Conclusion

It can be seen from Figs. 1 and 2 that defects can be clearly classified through the potential energy of atoms with different coordination. As can be seen in Figs. 1 and 2, the most numerous defects are the Si_5, Si_3, O_1 and O_3. All these defects have neighbors of opposite type.

As can be clearly observed in Fig. 3, the number of stable defects created generally increases with the initial energy of recoil atoms except for the case of Si_5 defects. This increase is larger for the case of O_1 (related to NBOC) and O_3 defects than for the case of Si_3 (related to ODCs and E' centers) defects.

Acknowledgments

This work has been performed under partial funding of Spanish National Project FNT2001-3886-C02-01 and European Union Keep in Touch Program on Inertial Confinement Fusion, and IAEACRP on element of power plants design for Inertial Fusion Energy. On of the authors (MJC) wants to thank the Ministerio de Educación y Ciencia in Spain for support under the Ramon y Cajal program.

References

[1] E.R. Hogdson, Nucl. Instrum. and Meth. B 191 (2002) 744.
[2] Jeffery F. Latkowski, Alison Kubota, Maria J. Caturla, Sham N. Dixit, Joel A. Speth, Stephen A. Payne, Fusion Sci. Technol. 43 (4) (2003) 540.
[3] C.D. Marshall, J.A. Speth, S.A. Payne, J. Non-Cryst. Solids 212 (1997) 59.
[4] R.A.B. Devine, Nucl. Instrum. and Meth. B 46 (1990) 244.
[5] F. Mota, M.-J. Caturla, J.M. Perlado, E. Dominguez, A. Kubota, J. Nucl. Mater. 329–333 (2004) 1190–1193.
[6] F. Mota, M.-J. Caturla, J.M. Perlado, E. Dominguez, A. Kubota, Fusion Eng. Des., in press.

[7] B.P. Feuston, S.H. Garofalini, J. Chem. Phys. 89 (9) (1988) 5818.
[8] MDCASK <http://www.llnl.gov/asci/purple/benchmarks/limited/mdcask>.
[9] A. Kubota, M.J. Caturla, J.S. Stolken, M.D. Feit, Opt. Express 8 (2001).
[10] P. Vashista, Rajiv K. Kalia, José P. Rino, Phys. Rev. B 41 (17) (1990) 12197.
[11] J. Molla, F. Mota, M. Leon, A. Ibarra, M.J. Caturla, J.M. Perlado, J. Nucl. Mater., these Proceedings, doi:10.1016/j.jnucmat.2007.03.192.